Full length article

Assessment of groundwater potentiality using geophysical techniques in Wadi Allaqi basin, Eastern Desert, Egypt – Case study

Ahmad Sobhy Helaly

Department of Geophysics, Faculty of Science, Ain Shams University, Egypt

ABSTRACT

Electrical resistivity surveying has been carried out for the determination of the thickness and resistivity of layered media in Wadi Allaqi, Eastern Desert, Egypt. That is widely used geophysical tool for the purpose of assessing the groundwater potential and siting the best locations for boreholes in the unconfined Nubian Sandstone aquifers within the study area. This has been done using thirteen 1D Vertical Electrical Sounding (VES) surveys. 1D-VES surveys provide only layered model structures for the subsurface and do not provide comprehensive information for interpreting the structure and extent of subsurface hydrogeological features. The integration of two-dimensional (2D) geophysical techniques for groundwater prospecting has been done to provide a more detailed identification for the subsurface hydrogeological features from which potential sites for successful borehole locations are recognized.

In addition, five magnetic profiles were measured for basement depth determination, expected geological structures and thickness of sedimentary succession that could include some basins suitable for groundwater accumulation as groundwater aquifers.

© 2017 Production and hosting by Elsevier B.V. on behalf of National Research Institute of Astronomy and Geophysics. This is an open access article under the CC BY-NC-ND license (http://creativecommons.org/licenses/by-nc-nd/4.0/).

1. Introduction

Wadi Allaqi study area lies within the longitudes 33°:08′E & 33°:21′E and Latitudes 22°:36′N & 22°:46′ N, in the Eastern Desert, Southern Egypt as shown in the location map (Fig. 1). To realize the potential of water availability, geophysical field measurements were done targeting the assessment of the groundwater availability in the Nubian Sandstone within the study area and siting the best boreholes locations for groundwater extraction.

Geophysical investigations provide a rapid and cost-effective means of developing information on subsurface hydrogeology (Kearey and Brooks, 1991). The use of geophysical methods for both groundwater resources mapping and water quality evaluation has increased dramatically over the last decades due to rapid advances in electronic technology and the development of numerical modeling solutions (Olayinka, 1991, Metwaly et al., 2009; Ndlovu et al., 2010). Although various hydro-geophysical tech-

niques are available, electrical resistivity is a popular method because of its low cost, simple operation and efficiency in areas with high contrasting resistivity, such as between the weathered overburden and the bedrock (Telford and Sheriff, 1990). Geoelectrical methods are particularly suitable for groundwater studies because the hydrogeological properties; such as porosity and permeability; can be correlated to electrical resistivity values. Geoelectrical techniques are essentially concerned with the measurement of electrical resistivities of subsurface materials, which preferentially provides information on the different geological layers, structures and the associated occurrence of groundwater (Stewart 1982, Van Overmeeren, 1989, Dahlin et al., 1999, Nowroozi et al. 1999; Meju, 2005). Also, resistivity is related to various geological parameters such as the mineral and fluid content, porosity, and water saturation rates.

2. Geologic setting

Geomorphologically, the study area is occupied by a number of valleys and is surrounded by mountains and highlands composed of complex basement rocks. Such valleys are mostly plains covered with sands, gravels and rock fragments. These valleys are gently sloping towards the southeast. From field observations, it is found that the deposited layers are also dipping towards the southeast.
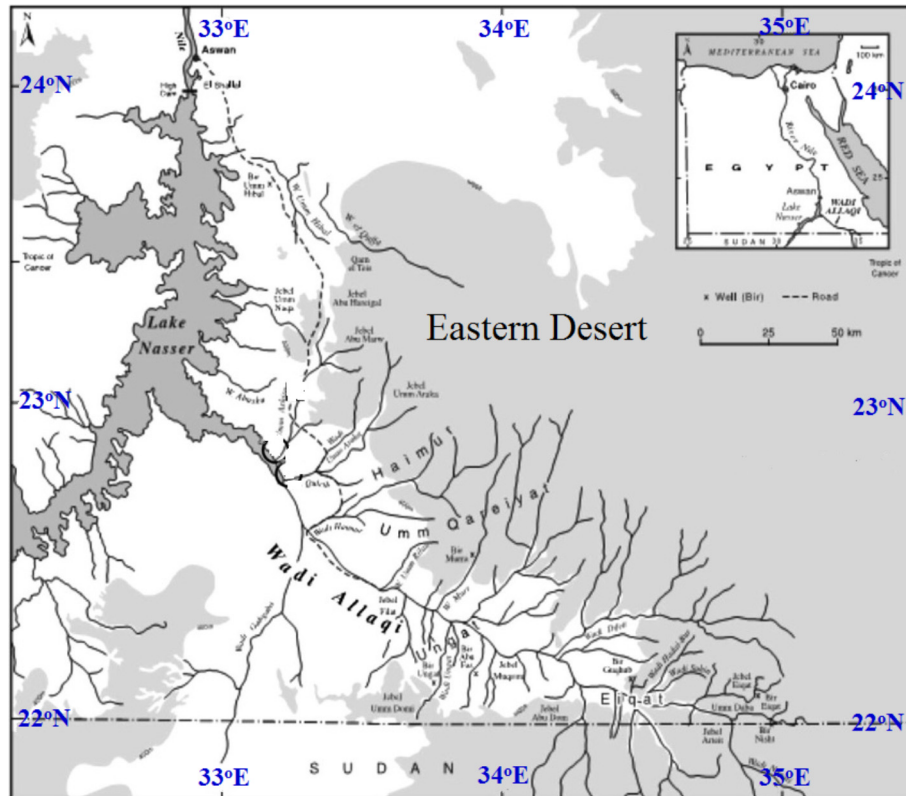
Production and hosting by Elsevier

Fig. 1. General location map of the study area & surroundings (Kandal et al, 2016).

Geologically, Wadi Allaqi is one of the most important valleys in the southern part of the Eastern Desert, to the east of Naser Lake. This valley is filled with fluvial sand and silt deposits belonging to Quaternary (Pleistocene) age. Fig. 2 shows a geological map illustrating that Wadi Allaqi is bounded by igneous and metamorphic rocks from the east, while from the west, it is bounded by Nubian Sandstone.

More enlightening information about the geology of the study area and its surroundings points to that, in general, about 50% of the granitic rocks in the Eastern Desert are classified as older and younger granites. The younger granites cover about 30% of the plutonic rocks in the Arabian shield. The relative abundance of the younger granites compared to the older granites increases from 1:4 due south of the Eastern Desert to about 1:1 due north (Stern
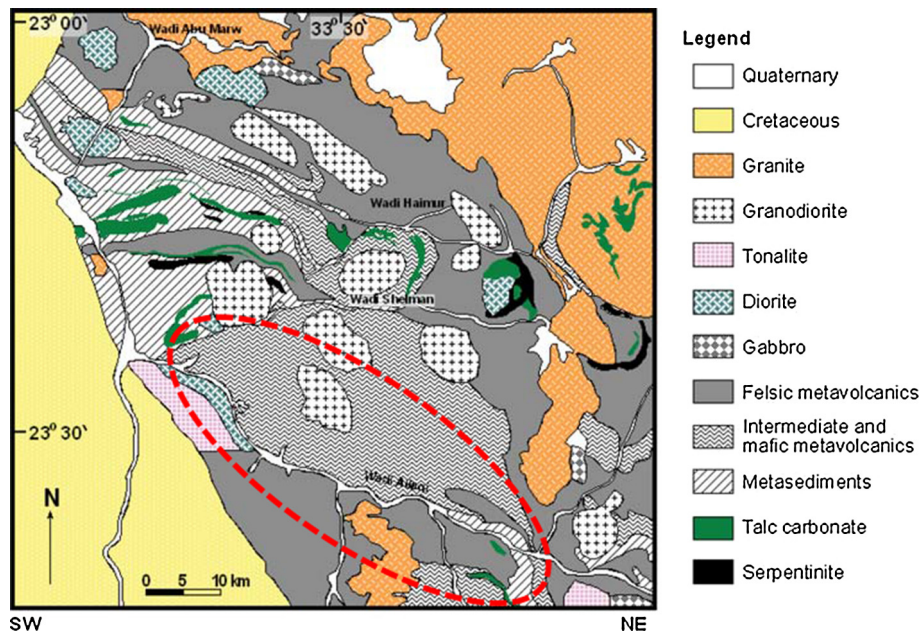

Fig. 2. Geological map of the study area (Wadi Allaqi) (Shams et al., 2012).

and Hedge, 1985). The hilly areas surrounding Wadi Allaqi (*Gabal Abu Marw, Gabal Haumor and Gabal um Shalman*) are related to the younger granite and late organic granite (El-Shazly, 1964). (*The word "Gabal" is the Arabic word for mountain*). These granites are younger than the surrounding country rocks represented by meta-sediments, meta-volcanic and meta-gabbro rocks.

The general geologic map of Wadi Allaqi area and surrounding areas is shown in Fig. 2.The rock varieties encountered from the oldest to the youngest are serpentines, talc carbonate, meta-sediments, meta-volcanic, metagabbro, gabbro, diorite granodiorite and Quaternary wadi deposits. This is with shear zone-associated auriferous quartz veins within ophiolitic-island arc metavolcanic terrains.

Also, Zoheir and Emam, (2012) compiled the geological and structural elements exposed in the mining sites within the Wadi Allaqi region, from integrated field, petrographic and satellite imagery data analysis as shown in Fig. 3. They mentioned that the study area is located within the Allaqi-Heiani belt in the South Eastern Desert of Egypt (Fig. 3). A highly tectonized, strongly foliated NW–SE-trending belt of interlayered ophiolites and island arc metavolcanic/volcaniclastic rocks dominates the area. This belt is cut by sheared and non-deformed granitoids intrusions. The ophiolitic rocks include serpentinite, metagabbro, metabasalt, and their highly sheared and metasomatized derivatives. The contact zone between metagabbro and serpentinite is defined by steeplydipping thrust structures, locally imposed by tight to isoclinal folds.

The study area (and its surroundings) subjected to several phases of deformation expressed by superimposed structures, including from older to younger:

(1). WNW-trending folds and antiforms and related foliations, commonly developed in the island arc metavolcanic rocks;
(2). NW- to NNW-trending, overturned folds and steeply-dipping, SE-vergent thrust segments and crenulation cleavage, common in ophiolitic rocks; and
(3). NNW-trending shear and mylonitic zones, quartz pods, conjugate sinistral NNW–SSE and dextral WNW–ESE strike-slip faults in the island arc and ophiolitic rocks everywhere in the study area and its surroundings.

The subsurface geologic setup was recently described by Khedr, et al. (2010) through their study of the stratigraphic rock units in and around Wadi Allaqi. Khedr, et al. (2010) suggested one formal "Group" of formation called the "**Nubia Group**". The clastic sequence which took place over the hard basement rocks including two un-official names of stratigraphic Groups or clusters of formations either underneath the Nubia Group (**Infra**) or overlying the Nubia Group (**Ultra**), (Fig. 4).
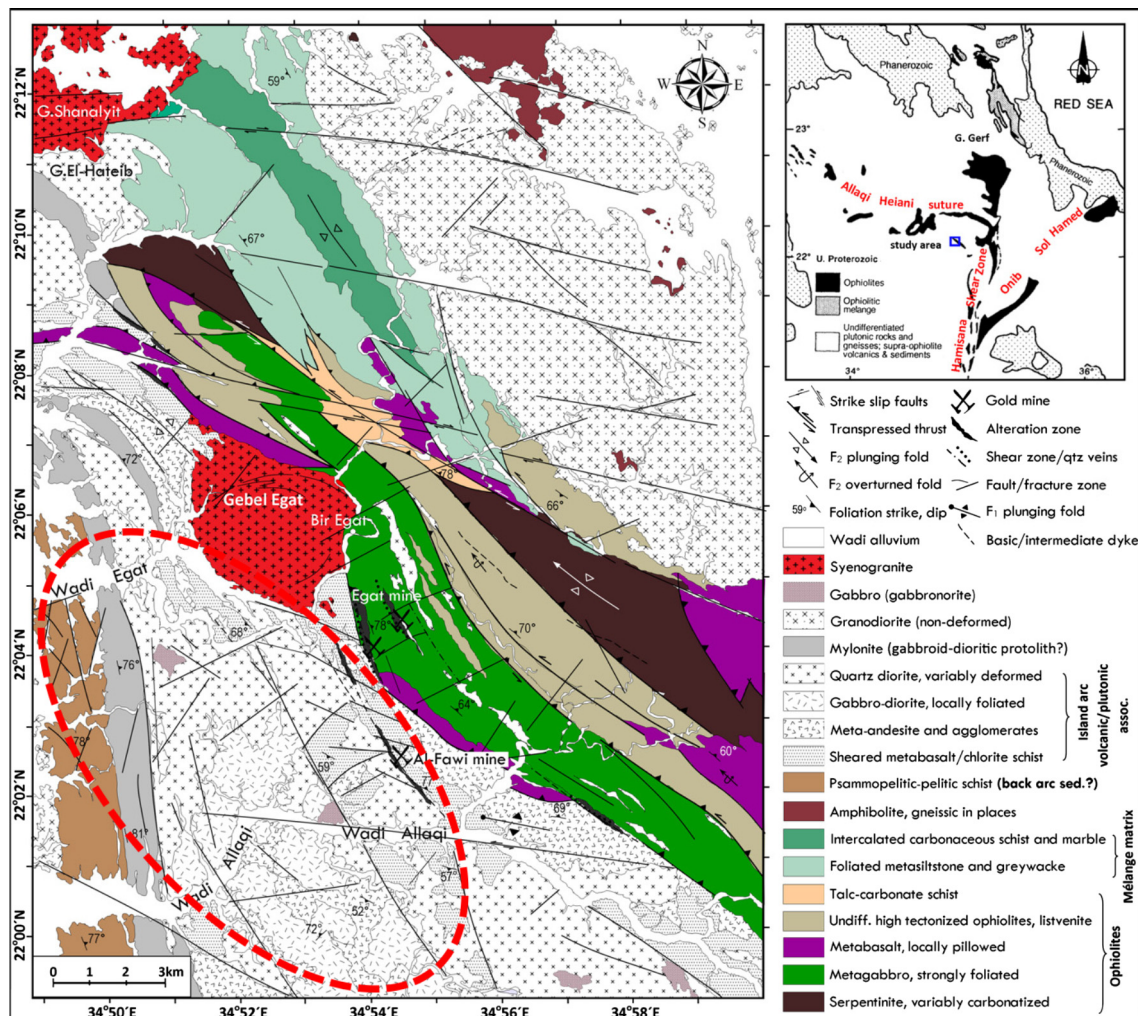

Fig. 3. Geological and structural elements exposed in the mining sites within the Wadi Allaqi region (Zoheir and Emam, 2012).
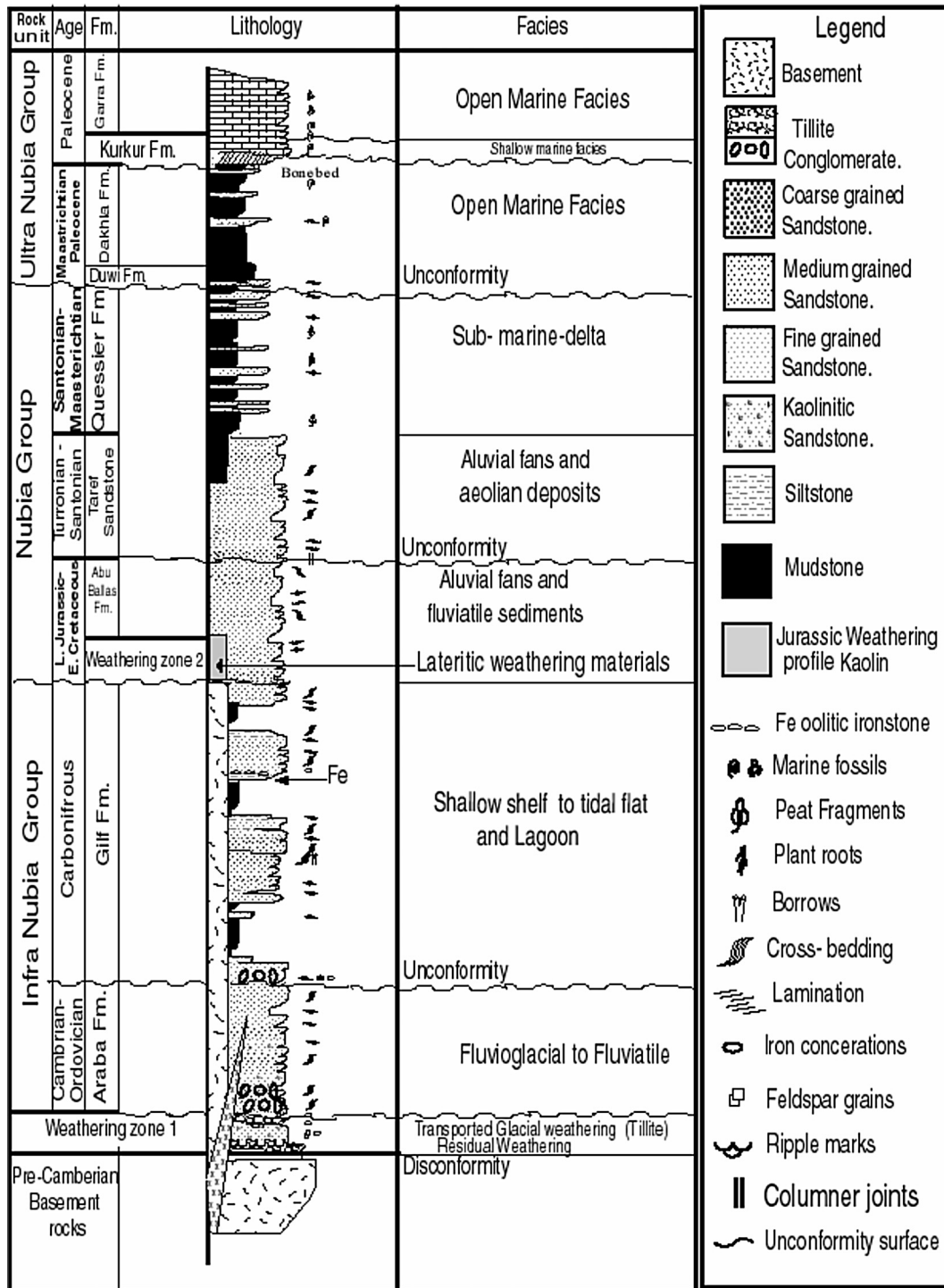
Fig. 4. Generalized stratigraphic section of the studied area (Khedr et al., 2010).

(1) The **Infra Nubia Group** includes all clastic rocks laid over the basement hard-rocks or their weathered zone. It represents sedimentary rocks ranging in age between Cambrian and pre-Late Jurassic age. This division includes four Paleozoic Formations, from base upward these are: Araba Fm., Gbgaba Fm., Naqus Fm., and Wadi Malik Fm. It also included the so called Abu Aggag Formation. The Infra Nubia sequence belongs to Ordovician-Silurian age and is made up of 400 m thick undisturbed and recycled glacio-fluvial sands and gravels, exposed near Gebel Uwainat at the southwestern corner of Egypt.

(2) The **Nubia Group** rock unit of Late Jurassic-Maastrichtian age and includes the Abu Ballas Formation, Taref Sandstone, Quseir Formation and covered by the "Maastrichtian-Recent" Ultra Nubia Group which started over the top of the Nubian Sandstone.

(3) The **Ultra Nubia Group** which includes all stratigraphic formations which took place since the early Paleocene and extends until the present time. The **Ultra Nubia Group** includes the Dakhla Formation, Esna Formation at the eastern bank of the Nile together with the coeval Paleocene age Kurkur and Garra Formations in the western side of the Nile as well as the followed upwards stratigraphic-formations in the study area.

3. Geophysical field measurements

3.1. Geoelectrical resistivity surveying

In this study, thirteen 1D vertical electrical soundings were conducted to conclude a subsurface resistivity model for assessing the availability of groundwater in the Nubian Sandstone Formation in Wadi Allaqi area, as shown in Fig. 4. The VES coordinates are given in Table 1.

The field work included the measurement of vertical electrical soundings in two locations using the SYSCAL R2 resistivity meter. This is through applying the Schlumberger configuration. It has been chosen because of its high efficiency for groundwater exploration. The layout (shown in Fig. 5) involved the current electrode spacing ($C_1C_2/2$) ranges from 75 m to 150 meters in first (southern) area and ranges from 200 m to 400 m in the second (northern) area. In the first area, there are two geoelectric profiles AB and

Table 1
VES's elevations and coordinates.

VES	Easting	Westing	Elevation
1	33° 15' 37.1″	22° 38' 09.3″	187
2	33° 15' 31.0″	22° 38' 07.5″	185
3	33° 15' 24.5″	22° 38' 02.6″	183
4	33° 15' 28.8″	22° 37' 57.3″	183
5	33° 15' 19.1″	22° 38' 07.4″	187
6	33° 15' 32.9″	22° 37' 50.2″	187
7	33° 15' 20.2″	22° 38' 14.6″	188
8	33° 14' 50.1″	22° 40' 34.9″	188
9	33° 14' 49.0″	22° 40' 59.1″	182
10	33° 14' 35.8″	22° 41' 59.8″	182
11	33° 13' 07.0″	22° 44' 28.9″	182
12	33° 14' 20.2″	22° 42' 27.4″	179
13	33° 14' 56.0″	22° 40' 27.4″	179

CD. The geoelectrical profile AB includes VES's 1, 2 and 3 as shown in Fig. 7, while profile CD includes VES's 4, 5, 6 and 7. The third geoelectric profile E-F was also conducted in the second area and composed of six VES's 8, 9, 10, 11, 12 and 13 as shown in Fig. 7. That is to measure the earth's resistivity (in ohm m) and measuring the earth's self-potential (SP) in mV/m as well (see Fig. 6).

This Schlumberger configuration is characterized by following up the vertical variations in the subsurface layers in each VES, together with horizontal variations through compiling and correlating the measured VES's along geoelectrical profiling.

3.2. Magnetic Surveying in the First Area/Location

Using a Proton Magnetometer (G-857) with an accuracy of 0.01 nT, five magnetic profiles were conducted in the first area with 110 measured magnetic stations in a detailed survey with station spacing 50–75 m covering an area of about 3.5 km^2. The station locations within each profile were traced using GPS with an accuracy of 0.01 m. Profiles#1 and #2 are trending NW-SE with lengths of 1.3 and 1.4 km, respectively, while Profile#3 is directed N-S with 2 km long, and Profiles #4 & #5 are oriented E-W with extensions of 1.3 and 1.5 km, respectively, as shown generally in Fig. 7. Another Proton magnetometer was placed at a fixed location and used as a reference base station magnetometer. It was adjusted to get a magnetic reading every 30 seconds. These readings were used to measure a diurnal variation that is used to estimate the diurnal correction in the study area.

4. Geophysical Interpretation

4.1. Geoelectrical resistivities interpretation

The geoelectrical survey helps in determining or concluding the conditions of the groundwater occurrence in the study area. To achieve this goal, the method of electrical resistance, which is one of the most important geophysical methods used to search for groundwater reservoirs, was used. The most important characteristics of this method is to determine the geometric dimensions of these groundwater reservoirs in terms of the thicknesses and depths of the water-bearing layers, from the earth's surface and the lithological contrast in the horizontal and vertical direction and the expected water salinity.
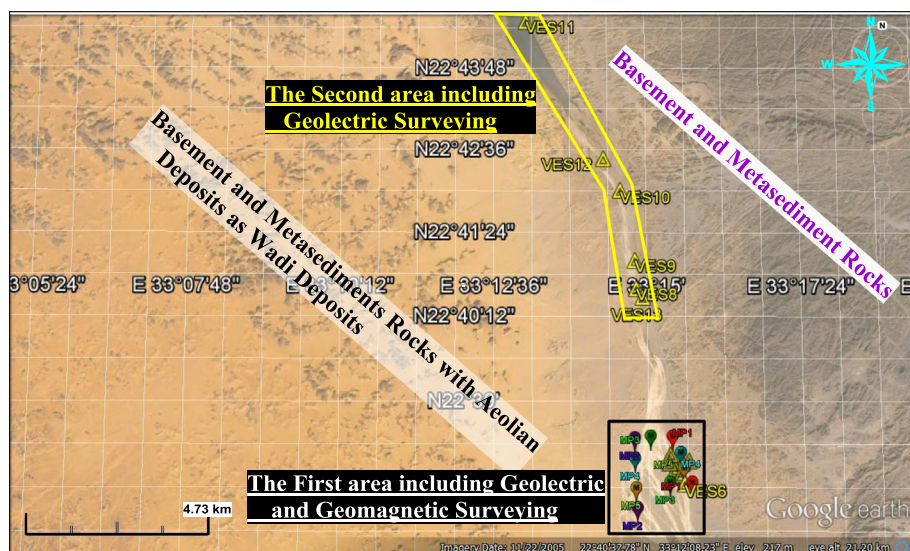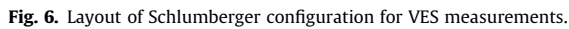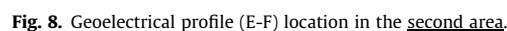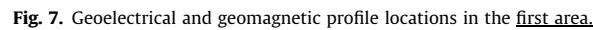

Fig. 5. Layout of the geophysical field measurements within the study area.

Fig. 6. Layout of Schlumberger configuration for VES measurements.

4.2. Interpretation of geoelectrical data in the <u>first area</u>

Based on the field-measured geoelectrical data; in the form of apparent resistivity for subsurface sequences versus the electrode spacings; the Rinvert-32 software was used to conclude the number of subsurface geological layers and their geoelectrical properties, and whether they contain water or not.

4.2.1. The Geophysical Profiles

In the first area, the measured geophysical probes (shown in Figs. 8 and 10) were used in the geophysical profiling work. One of which is the longitudinal profile (A–B) and the other is transverse profile (C–D). Their inverse modeling is shown in Figs. 8 and 10. That is to illustrate the vertical and horizontal variations of the possible geological formations, and also to elucidate the presence of conducting water in these layers, depending on its
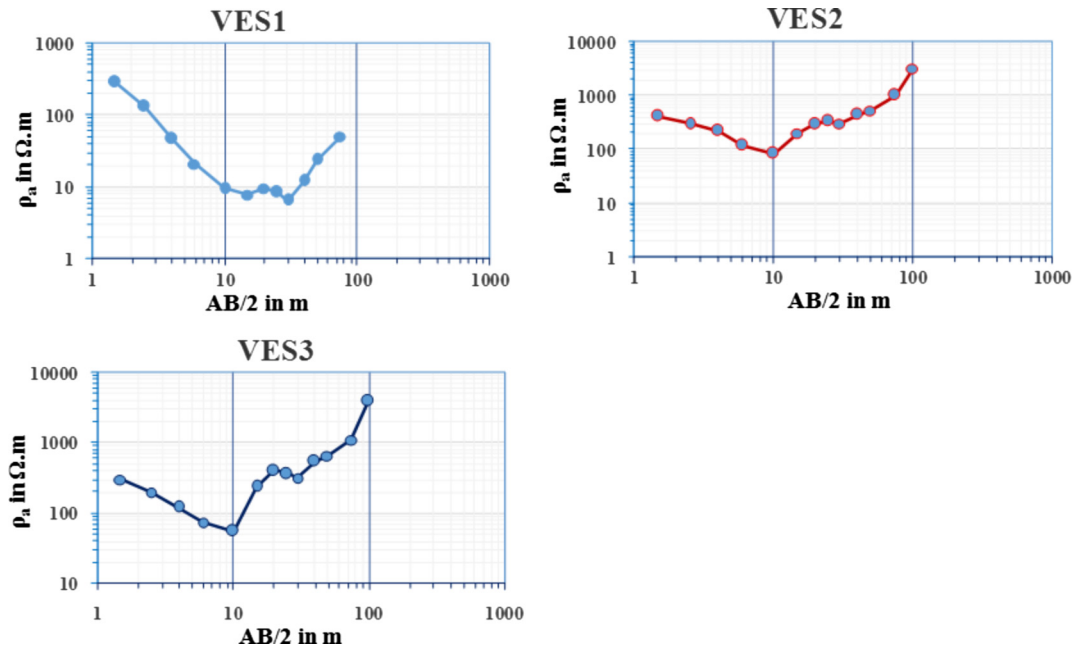

Fig. 7. Geoelectrical and geomagnetic profile locations in the <u>first area.</u>

Fig. 8. Geoelectrical profile (E-F) location in the <u>second area</u>.

Fig. 9. The VES curves for the Geoelectrical Profile A-B.

influence on the electric current as a good electrical conductor. Accordingly, the different depths *to the upper or to the lower surfaces of these sequences* can be determined.

4.2.1.1. Description of the geoelectrical layers in the first area. The interpreted subsurface geological units in the first area (Figs. 10 and 12) could be divided into two different geological layers based on their true electrical resistance, as well as their thicknesses as interpreted from the data profiles (Figs. 9 and 11). The upper part of this sequence belongs to the Quaternary age and is composed of the surface layers of the wadi deposits, which are gravel, sand and silts with mixtures of rock fragments and sand. The lower part of

this sequence belongs to the Cambrian age and is generally represented by the rocks of basement complex and metamorphosed sedimentary rocks.

The details of the electrical properties of these geological sequences are as follows:

(i) The first geoelectrical layer

Is a layer of surface gravel, sand, silt and rock fragments, which is called the wadi deposits with a significant increase of silt and vary in electrical resistivity of around 15 ohm m at the bottom of this horizon (due to the increasing water content) to about
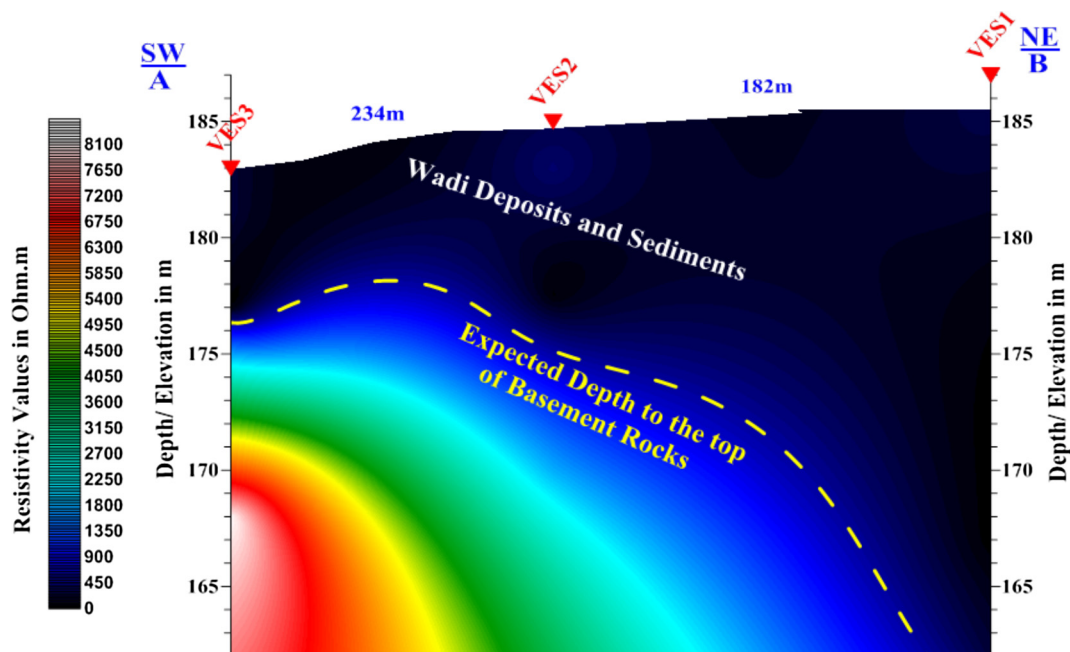

Fig. 10. The Inverse model for the interpreted VES curves for the Geoelectrical Profile A-B, along with the interpreted geological units.
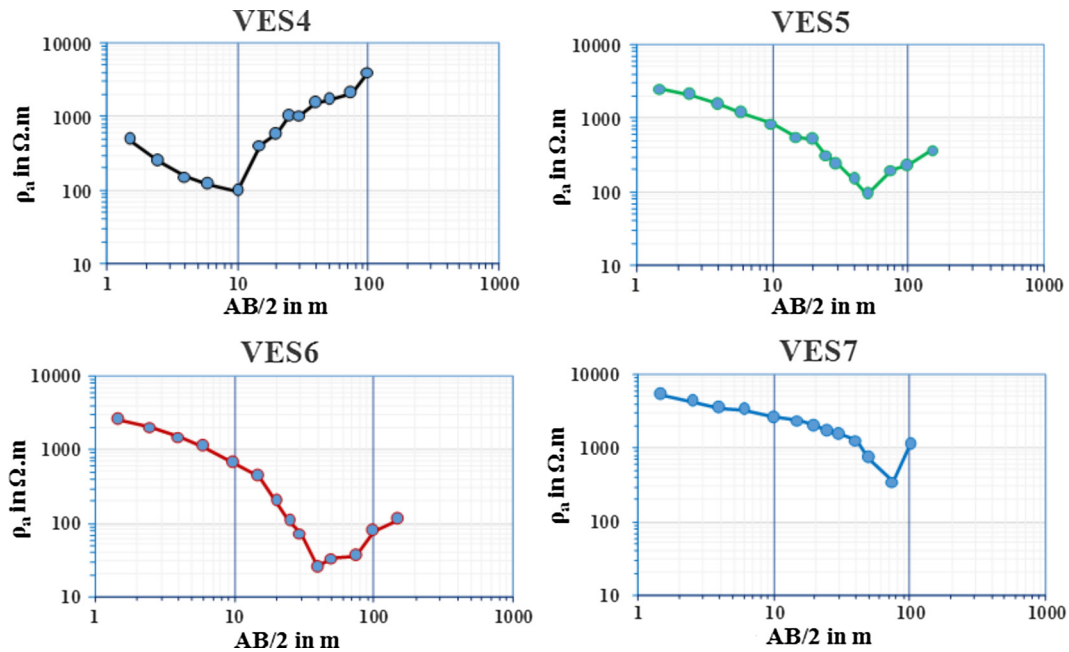
Fig. 11. The VES curves for the Geoelectrical Profile C-D.

5169 ohm m in the upper parts of this layer. This is with a thickness that ranges from 6 meters to about 25 meters. The general resistivity values of this layer indicate that they are dry, in general, towards the top.

  (ii) The second geoelectrical layer

  Is a layer with relatively higher resistivity of about 231 ohm m (due to the effect of the upper silty layer) and also is affected by some erosional factors and reached resistivity values of more than 11000 ohm m; downwards. Originally, it is a unit of hard rock consisting of basement rocks and metamorphosed sedimentary rocks. And the depth of this horizon is starting from the depths of 6 meters to about 25 m in and around some places of the study area.

4.2.1.2. Description of the geoelectrical layers in the Second Location. Fig. 8 is a map showing the second location in the study area and the distribution of VES soundings (8, 9, 10, 11, 12, and 13) is along the profile E-F in this area. Fig. 12 shows the field curves and the calculated curves of these VES's along this profile.

  Four electrical layers in the second location were found with different true resistivities and thicknesses as shown in Figs. 13 and 14. The upper surficial part of the geological section in this area belongs to the Quaternary age and consists of Wadi deposits of gravel, sand with rock fragments followed by sand and silt intercalations. While the lower part represented the Precambrian Era composes of fractured metasediments followed downwards by hard basement rocks.(SeeFig. 15)
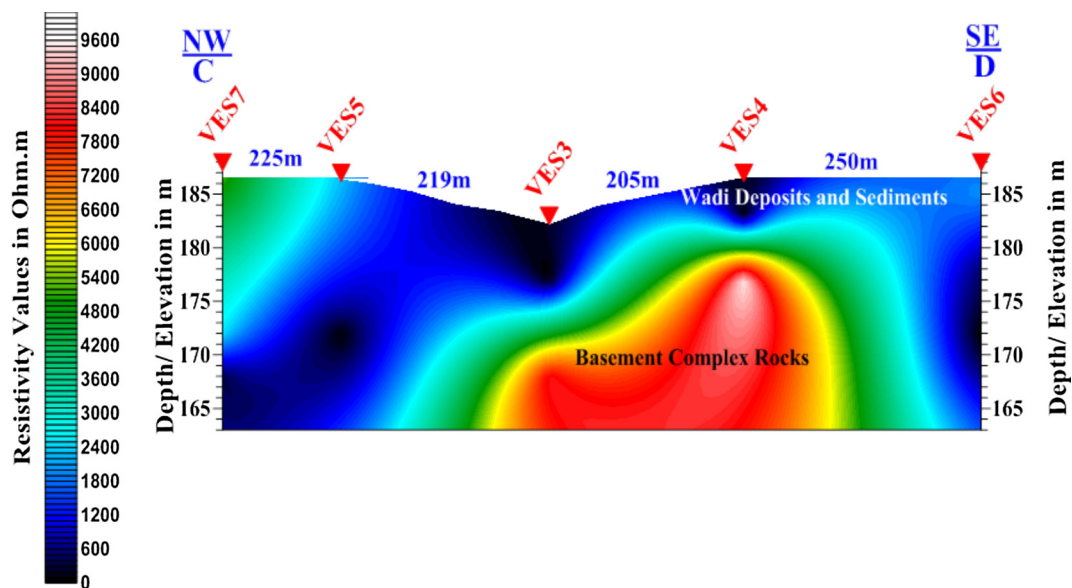

Fig. 12. The Inverse model for the interpreted VES curves of the Geoelectrical Profile C-D, along with the interpreted geological units.
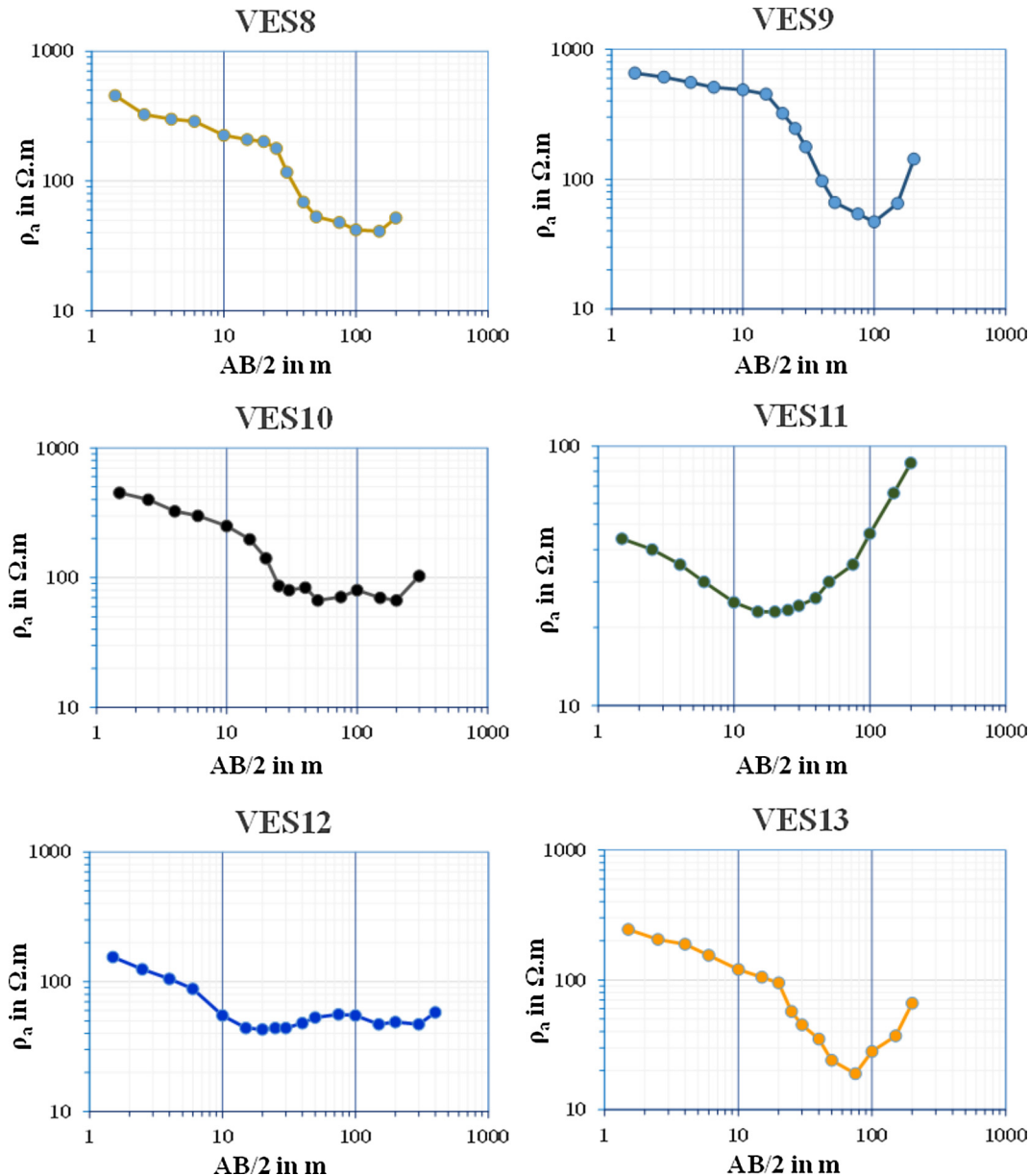
Fig. 13. The VES curves for the Geoelectrical Profile E-F.

(i) The first geoelectrical layer

It is a surficial layer with true resistivities varied from 44 Ohm m at VES 11 to 725 Ohm m at the VES's far away from the Naser Lake; and with a range of thickness between 1–9 meters. This layer is composed of dry Wadi deposits of sands and gravels with rock fragments.

(ii) The second geoelectrical layer

It is an extension of the surficial layer composed also of sands and gravels with silt intercalations. The true resistivity values lie in the range of 22–51 Ohm m at VES's 10, 11 and 12 with thickness range of 17.5–29.5 m. This layer is probably saturated with groundwater at this part. While it provides electrical resistivities in the range of 119–258 Ohm m at VES's 8, 9 and 10 with thickness range 8–12 meters indicating that is dry at that part.

(iii) The third geoelctrical layer:

This layer is probably formed of fractured rocks that might contain groundwater. This was noticed from the deduced electrical resistivity values which range from 12 to 38 Ohm m. This indicates moderate to high fracture density with a thickness of about 32–39 meters. Lower to moderate fracture density also exists in this layer below the two VES's V#10 and V#12. This was deduced from the obtained geoelectrical resistivity values which range from 80 to 150 Ohm m, and a thickness varies from 21 to 24 meters.

(iv) The fourth geoelctrical layer

This layer is characterized by resistivity values that range from 114 to 1073 Ohm m. It is expected to be of hard basement rocks' nature, or highly metamorphosed sedimentary rocks. Most likely, this layer is located at a depth range from 47 to 90 meters below the earth's surface.
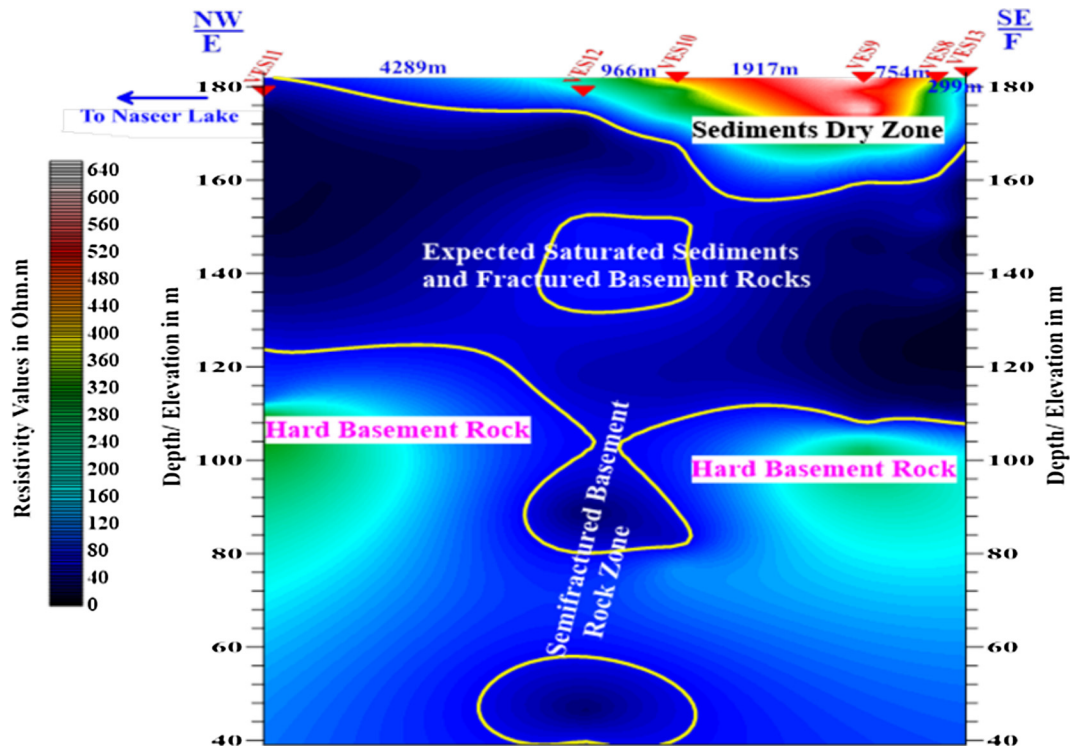
Fig. 14. The forward (preliminary) model of the calculated VES curves for the Geoelectrical Profile E-F, along with the expected geological units.
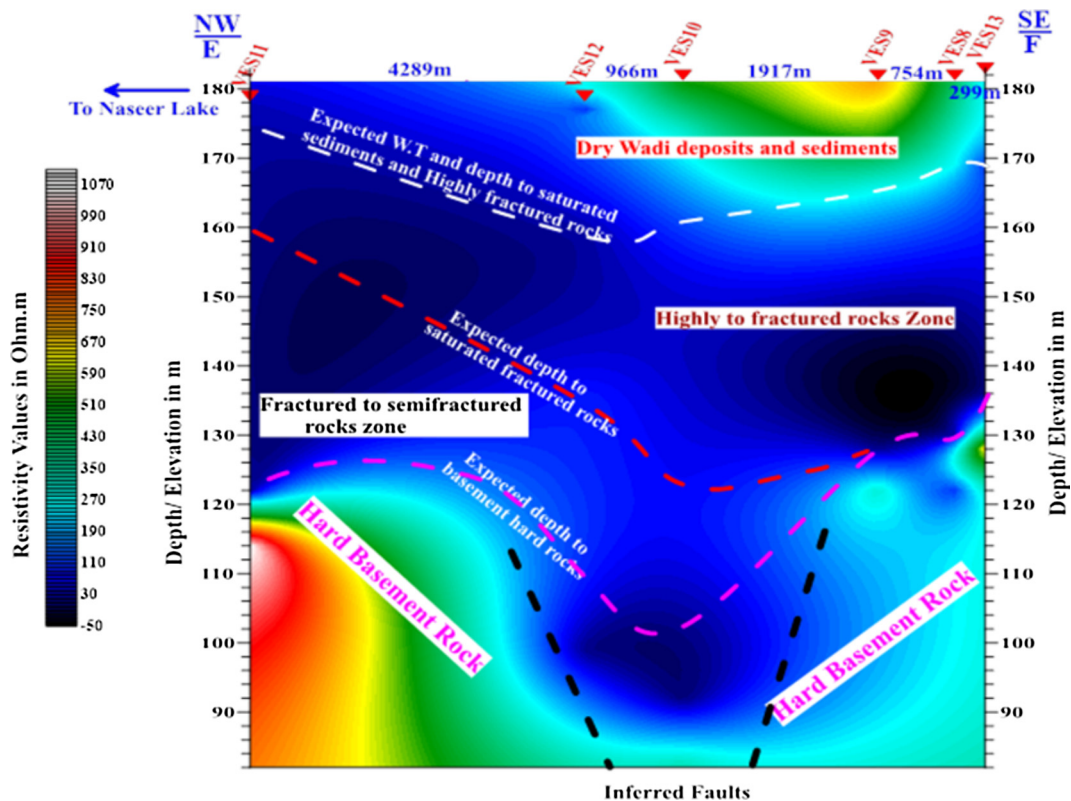

Fig. 15. The Inverse model for the interpreted VES curves for the Geoelectrical Profile E-F, along with the interpreted geological units.

4.2.1.3. Interpretation of Self-Potential Measurements in the Second Area. Self-potential (SP) technique is usually used as an assisting tool in expecting the locations groundwater accumulation, axes of drainage and the direction of water flow. Fig. 16 shows SP curves measured along profile E-F in the second area. After correlation of the SP curves with the VES's 8, 9, 10, 11, 12 and 13 curves, it was
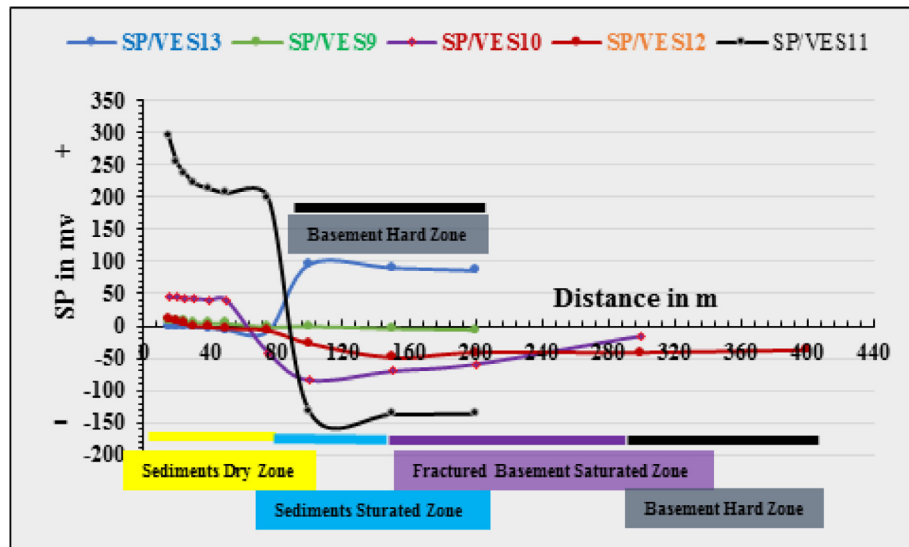
Fig. 16. Distribution of SP data and curves along the Profile E-F with the expected geological units.
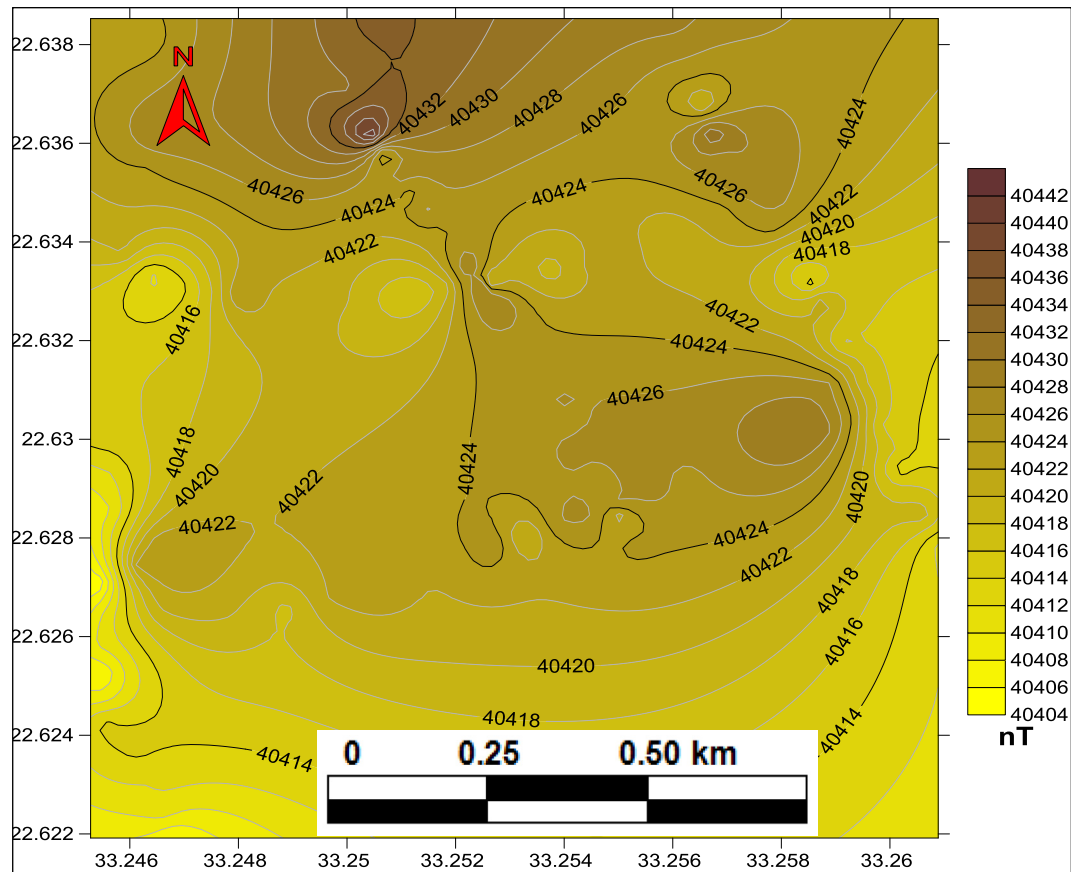

Fig. 17. Corrected total magnetic intensity map in the study area.

found that there are some positive SP values representing the surficial dry deposits and hard basement rocks, while the negative SP values representing the groundwater saturated deposits and fractured rocks.

4.2.1.4. Interpretation of Geomagnetic Data in the First Area. The objectives of any geomagnetic study are the determination of depth to the basement surface; i.e. the thickness of the sedimentary cover,

structural elements configuration (major and minor faults), delineation and identification of the borders of the sedimentary basins and their extensions that represent the main groundwater aquifers. Hence, the best locations for drilling groundwater boreholes can be assessed. Moreover, the occurrence of igneous intrusions like dykes and sills can be identified, which affect the possibility of groundwater flow within the aquifers. The locations of these intrusions should be determined by magnetic studies to assist the drilling operation.
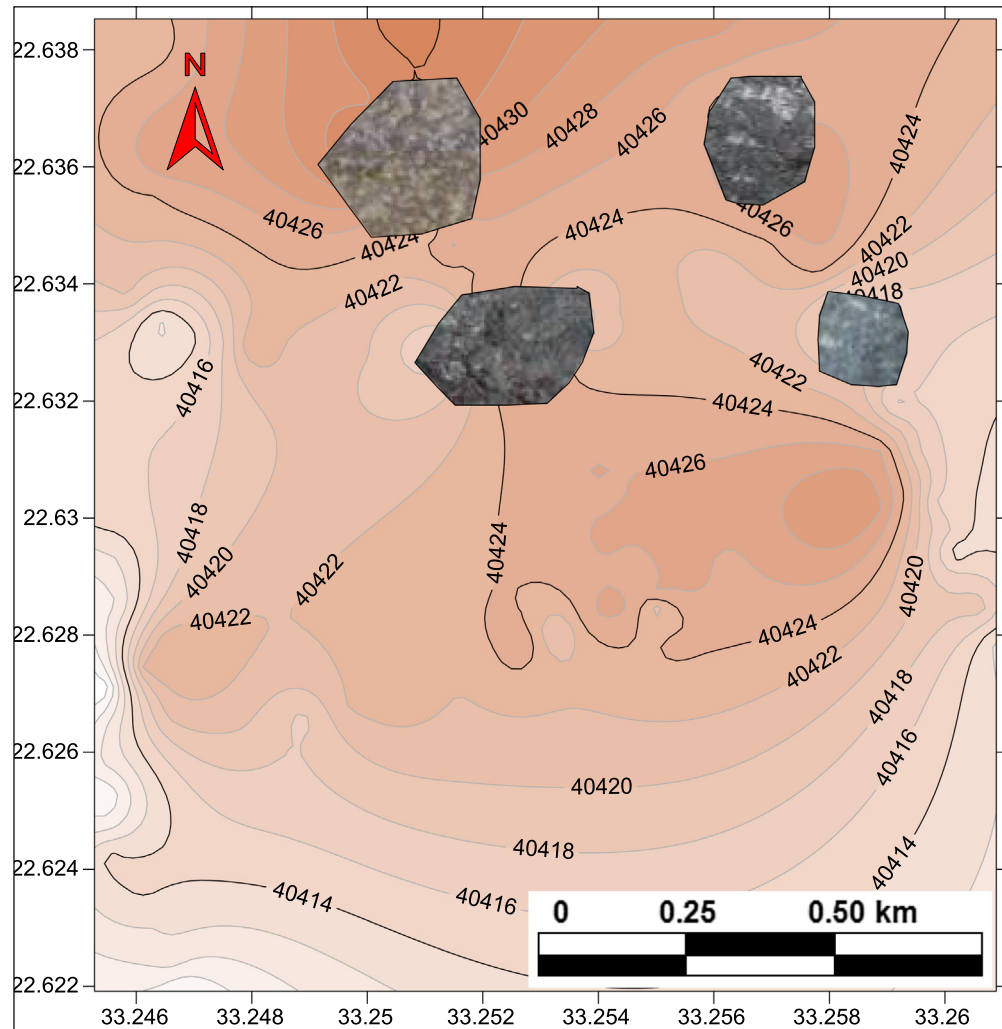
Fig. 18. Arial Locations of expected igneous intrusives within the first location area.

Fig. 17 represents the corrected total magnetic intensity map; showing values range from 40404.7 to 40442.1 nT with a difference range of 37.4 nT, while the mean value is about 40423.1 nT.

The lower values (with negative polarity) are found within the southeastern and southwestern parts of the study area, while, higher values (with positive polarity) are found within the central and northern parts. Also, no clear faults were detected within the study area.

Fig. 17 shows a number of circular anomalies of dipolar nature indicating some possible igneous intrusions existed in the study area. From the map, it can be concluded that there is a number of alternating positive and negative magnetic anomalies of different extensions. The positive broad magnetic anomalies indicate structural basement highs (swells) that represent thin and shallow sedimentary cover. While the negative anomalies indicate structural basement lows (troughs) representing deeper sedimentary succession of larger areal extension that are more suitable for groundwater accumulation and represent the best locations for boreholes drilling in the unconfined Nubian Sandstone aquifer. Fig. 18 shows the aerial locations of expected igneous intrusive bodies within the first location area.

A sub-basin, in the form of an extended-tongue, was noticed within the main basin in the southwestern part of the study area. This sub-basin was formed as a down-warped local depression within the low-lying basement rocks which made better location for more sediment to be deposited within this part. Therefore, it is expected that this sub-basin has a greater thickness of Nubian Sandstone deposits.

Fig. 19 is a map showing the depth distribution to basement surface. The basement depth is in the range of 80–100 m with deeper values inside the main basin in the southwestern part attaining 100 m, while these values reach 80–85 m in northern and northeastern parts.

In summary, geomagnetic investigations indicated that there are several magnetic intrusions in the central and northern parts and great thickness of the sedimentary sequence is found in the southern and southwestern parts that could be selected for siting the best locations for groundwater borehole drilling.

5. Summary and conclusions

Geophysical field measurements in terms of VES surveying, magnetic data and SP and have been used in two separate areas in Wadi Allaqi study area, aiming at the detecting of groundwater potential and siting the locations for drilling boreholes.

In the first study area, the shallow part of the geological section is divided into two different geoelectric layers. The first surficial layer belongs to the Quaternary age and it is composed of dry gravel, sand, silt and rock fragments with a thickness range of
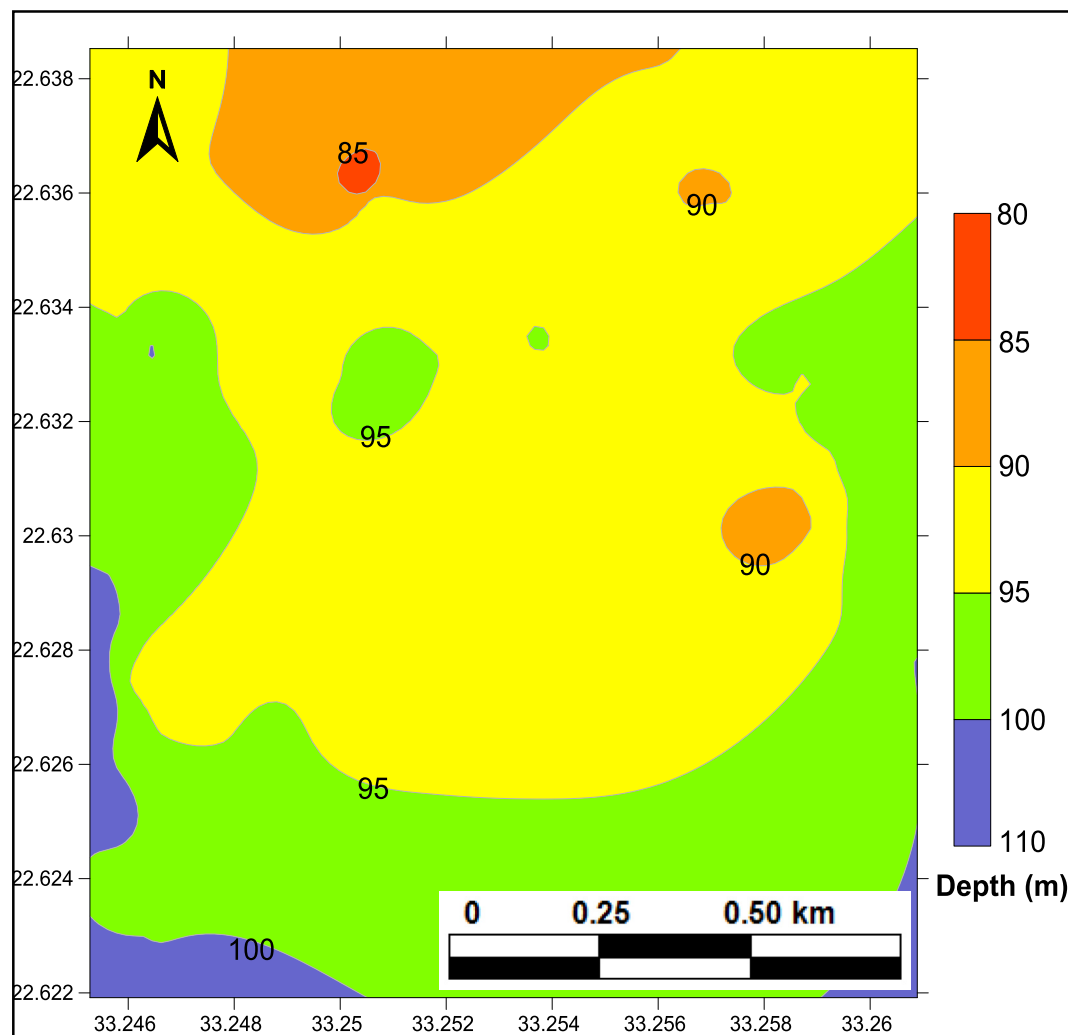
Fig. 19. Depth to the basement surface relief map.

about 6 to 25 meters, which is also, confirmed from magnetic interpretation. The second geoelectrical unit is composed of metamorphosed sedimentary rocks or basement-nature rocks with higher resistivity values.

In the second area, four geoelectrical layers were found with different interpreted true resistivities and thicknesses. The upper surficial part of the geological section in this area belongs to the Quaternary age and consists of Wadi deposits of gravel, sand with rock fragments followed by sand and silt intercalations. The lower part represents the Precambrian Era and is composed of fractured metasediments followed downwards by hard basement rocks.

The groundwater potential is expected in the second electrical layer near VES's 10, 11 and 12 that is composed of sands and gravels with silt intercalations of lower resistivity values and ranges in thickness from 17.5 to 29.5 meters. And, the groundwater occurrences could also be expected in the third unit, which is formed of fractured rocks due to its noticeable lower resistivities with a thickness of about 32–39 m.

Self-potential work assisted in confirming the above-mentioned results of VES's interpretation through expecting the locations groundwater accumulations along profile E-F in the second area. The negative SP values representing the groundwater saturated deposits and fractured rocks were found near VES's 10 and 12 with depths in the range of 2 meters (close to lake) to 20 meters (far from the lake).

It is worth to be mentioned that, based on the concluded geophysical studies and also, the field observations mentioned above; that two boreholes can be drilled for groundwater usage from this aquifer which is characterized by its high potentialities, especially in the second area. The best locations for these boreholes are close to VES's 10 and 12 along profile E-F in the second area with depth down to about 75 meters. Also, pumping tests can be carried out for estimating the hydraulic parameters for clarifying the safe production rates and whether both wells can be used simultaneously or mutually.

References

B. Zoheir A. Emam 2012 Integrating geologic and satellite imagery data for high-resolution mapping and gold exploration targets in the South Eastern Desert, Egypt J. Afr. Earth Sci. 66–67/22–34.

Dahlin, T., Jens, E., Dowen, R., Mangeya, P., Auken, E., 1999. Geophysical and hydrogeologic investigation of groundwater in the Karoo stratigraphic sequenceat Sawmills in northern Matabeleland, Zimbabwe: a case history. Hydrogeol. J 15 (5), 945–960.

El-Shazly, M.E., 1964. On the classification of the Precambrian and other rocks of magmatic affiliation in Egypt. Ann. Geol. Surv. Egypt IV, 125–135.

Kandal, Hanaa A., Yacoub, Hoda A., Gerkema, Menno P., Swart, A.A. Jac, 2016. Vanishing knowledge of plant species in the Wadi Allaqi desert Area of Egypt. Hum Ecol 44, 493–504.

Kearey, P., Brooks, M., 1991. An Introduction to Geophysical Exploration. Oxford Publishing House, Blackwell Scientific.

Khedr, E.S., Youssef, A.A.E., Abou Elmagd, K., Khozyem, H.M., 2010. Tectono-stratigraphic subdivision of the clastic sequence of Aswan area, southern Egypt. In: Fifth International Conference on the Geology of the Tethys Realm, South Valley University, January 2010, pp. 197–216.

Meju, M., 2005. Simple relative space–time scaling of electrical and electromagnetic depth sounding arrays: implications for electrical static shift removal and joint DC TEM data inversion with the most-squares criterion. Geophys. Prospect. 53, 1–17.

Metwaly, M., El-Qady, G., Massoud, U., El-Kenawy, A., Matsushima, J., Al-Arifi, N., 2009. Integrated geoelectrical survey for groundwater and shallow subsurface evaluation: case study at Siliyin spring, El-Fayoum. Egypt. Int. J. Earth Sci. 99, 1427–1436.

Ndlovu, S., Mpofu, V., Manatsa, D., Muchuweni, E., 2010. Mapping groundwater aquifers using dowsing, slingram electromagnetic survey method and vertical electrical sounding jointly in the granite rock formation: a case of Matshetshe.

Nowroozi, A.A., Horrocks, S.B., Henderson, P., 1999. Saltwater intrusion into the freshwater aquifer in the eastern shore of Virginia: a reconnaissance electrical resistivity survey. J. Appl. Geophys. 42, 1–22.

Olayinka, A.I., 1991. Geophysical siting of boreholes in crystalline basement areas of Africa. J. Afr. Earth Sci. 14 (2), 197–207.

Issa, Shams A.M., Uosif, M.A.M., Abd El-Salam, L.M., 2012. Natural radionuclide concentrations in granite rocks in Aswan and central-Southern Eastern Desert, Egypt and their radiological implications. Radiat. Prot. Dosimetry 150 (4), 488–495.

Stern, R.J., Hedge, C., 1985. Geochronological and isotopic constraints on late pressure crustal evolution in the Eastern Desert of Egypt. Am. J. Sci. 285, 97–172.

Stewart, M.T., 1982. Evaluation of electromagnetic methods for rapid mapping of salt water interfaces in coastal aquifers. J. Ground Water 20, 538–545.

Telford, E., Geldart, W.M., Sheriff, R.E., 1990. Applied Geophysics. Cambridge University Press, UK.

Van Overmeeren, R., 1989. Aquifer boundaries explored by geoelectrical measurements in the coastal plain of Yemen. A case of equivalence. Geophysics 54, 38–48.